



OPEN ACCESS

EDITED BY

João P. Leite,
University of São Paulo, Brazil

REVIEWED BY

Xinglin Zeng,
University of Maryland, United States
Jose Eduardo Peixoto-Santos,
Federal University of São Paulo, Brazil

*CORRESPONDENCE

Agnieszka Olejnik
✉ an.olejnik@uw.edu.pl

RECEIVED 08 January 2025

ACCEPTED 09 July 2025

PUBLISHED 14 August 2025

CITATION

Olejnik A, Bala A, Rejner W,
Gottman-Narożna A, Rysz A,
Kopytek-Beuzen M, Naumczyk P and
Kunert P (2025) Gray matter abnormalities
and memory impairment in left mesial
temporal lobe epilepsy.
Front. Hum. Neurosci. 19:1554091.
doi: 10.3389/fnhum.2025.1554091

COPYRIGHT

© 2025 Olejnik, Bala, Rejner,
Gottman-Narożna, Rysz, Kopytek-Beuzen,
Naumczyk and Kunert. This is an
open-access article distributed under the
terms of the [Creative Commons Attribution
License \(CC BY\)](#). The use, distribution or
reproduction in other forums is permitted,
provided the original author(s) and the
copyright owner(s) are credited and that the
original publication in this journal is cited, in
accordance with accepted academic
practice. No use, distribution or reproduction
is permitted which does not comply with
these terms.

Gray matter abnormalities and memory impairment in left mesial temporal lobe epilepsy

Agnieszka Olejnik^{1*}, Aleksandra Bala¹, Weronika Rejner²,
Antonina Gottman-Narożna², Andrzej Rysz³,
Maja Kopytek-Beuzen², Patrycja Naumczyk⁴ and
Przemysław Kunert²

¹Faculty of Psychology, University of Warsaw, Warsaw, Poland, ²Department of Neurosurgery, Medical University of Warsaw, Warsaw, Poland, ³Department of Neurosurgery, 1 Military Clinical Hospital with Outpatient Clinic: Lublin, Subsidiary in Ełk, Ełk, Poland, ⁴University of Gdańsk, Gdańsk, Poland

Objectives: Mesial temporal lobe epilepsy (MTLE) is a common neurological disorder, with memory impairment being one of its typical symptoms. Most previous studies have focused on assessing declarative memory directly related to hippocampal functions, but emerging data suggest a decline in the efficiency of other types of memory as well. The aim of this study was to comprehensively assess various types of memory and analyze the relationship between memory performance and the volume of selected gray matter structures.

Methods: In total, 21 patients with left-MTLE and 28 age- and education-matched healthy individuals underwent neuropsychological assessment using the Wechsler Memory Scale IV (WMS-IV) to evaluate memory functioning. Magnetic resonance imaging was also conducted to assess gray matter volume and structure in all participants.

Results: Compared with healthy controls, patients with left-MTLE showed significantly reduced performance in short-term verbal and visual memory, long-term verbal and visual memory, and working memory. Volumetric analysis revealed differences in gray matter volume between groups, with some structures being smaller and others larger in the patient group. Numerous correlations were found between WMS-IV scores and the volume of specific brain regions. Significant associations were observed both ipsilateral and contralateral to the epileptic focus, involving regions such as the cerebellar cortex, cingulate gyrus, insula, thalamus, and pallidum.

Conclusion: This study expands our understanding of the memory profile in patients with MTLE. Neuropsychological testing showed that patients performed worse than controls across all assessed memory domains. Additionally, the study identified a distinct pattern of neuronal abnormalities and brain-behavior correlations. These findings suggest that the extent of structural brain anomalies may be linked to the severity of memory impairment in MTLE, underscoring the complex relationship between neuroanatomy and cognitive function in this population.

KEYWORDS

mesial temporal lobe epilepsy (MTLE), left mesial hippocampal sclerosis, memory deficits, short-term memory, long-term memory, working memory, gray matter, volumetry

1 Introduction

Mesial temporal lobe epilepsy (MTLE) is a common type of epilepsy, often caused by hippocampal sclerosis and frequently resistant to antiepileptic drugs (Ryvlin et al., 2014; Siemianowski and Królicki, 2005; Kwan and Sander, 2004). The mesial portion of the temporal lobe is strongly associated with memory, as evidenced by numerous studies documenting mnemonic impairment in this patient population (Butler and Zeman, 2008; Rayner et al., 2016; Zhu et al., 2021). Although seizures originate in a specific focus, they may impact the structure and function of the entire brain because epilepsy is a network disease (Bonilha et al., 2012). This has been demonstrated by studies identifying neural damage extending beyond the hippocampus to regions such as the amygdala and parahippocampal gyrus (Dos Santos Silva et al., 2024; Zheng et al., 2018; Pail et al., 2010), as well as the corpus callosum, prefrontal cortex, thalamus, caudate nucleus, cingulate gyrus, and insula (Dos Santos Silva et al., 2024; Zheng et al., 2018; Bonilha et al., 2012). Therefore, structural changes in patients with MTLE are not limited to the mesial temporal lobe but can also be found throughout the brain, even in the hemisphere opposite the epileptic focus (Pail et al., 2010; Bonilha et al., 2012). As a result, patients experience a range of difficulties beyond memory impairment, including deficits in executive functions, attention, language, social cognition, and more (Olejnik et al., 2024; Zhou et al., 2019; Bell et al., 2003; Bala et al., 2024; Ives-Deliperi and Butler, 2021). Memory deficits, in particular, cannot be explained solely by changes in the hippocampus because memory is a highly complex construct. There is no single brain region responsible for all memory processes.

Memory is a complex and broad concept, encompassing many subtypes. However, in this study, we focused on specific types of memory: short-term verbal memory, short-term visual memory, long-term verbal memory, long-term visual memory, and working memory.

Epileptic seizures may be related to structural changes in the brain, with a potentially bidirectional relationship between the two variables. These structural alterations, in turn, may correlate with the clinical presentation and cognitive impairment profiles of patients. Several studies have shown that seizures can disrupt various types of memory (Butler and Zeman, 2008; Rayner et al., 2016; Zhu et al., 2021; Caciagli et al., 2023). Therefore, when assessing patient functioning, it is important to look beyond the most obvious and frequently studied domain—declarative long-term memory (Ono et al., 2021; Zheng et al., 2018; Butler and Zeman, 2008)—and expand the diagnostic protocol to include tasks that evaluate other types of memory. It is also essential to assess memory in at least two modalities: verbal and visual. Given the breadth and complexity of the memory construct and its various subtypes, this study was designed to allow for a comprehensive examination of memory. In light of potential structural abnormalities, we also conducted volumetric analyses of gray matter in patients' brains, measuring the volume of individual regions. These measurements were then used for both comparative analyses (with a group of healthy individuals) and

correlational analyses (with results from comprehensive memory assessments).

The aims of this study were to comprehensively evaluate various aspects of memory in patients with drug-resistant MTLE and compare them with healthy subjects, to correlate memory performance with the volume of specific brain structures, and to examine the relationship between memory performance and clinical factors such as age at epilepsy onset and duration of epilepsy.

2 Materials and methods

2.1 Participants

In total, 31 patients diagnosed with MTLE and 28 healthy controls participated in this study. Patients were recruited from the Department of Neurosurgery at the Medical University of Warsaw during hospitalization. The diagnosis of MTLE was confirmed by an experienced epileptologist based on seizure semiology, video-electroencephalography, and magnetic resonance imaging (MRI) findings that revealed hippocampal abnormalities suggestive of hippocampal sclerosis. The control group was recruited through a social media announcement. Healthy individuals were matched with the clinical group in terms of age and level of education. The exclusion criteria were the presence of metal elements in the body or claustrophobia preventing MRI examination; significant visual, auditory, or motor impairments that could interfere with neuropsychological testing; neurological diseases (other than epilepsy in the clinical group); use of medications affecting the central nervous system (excluding antiepileptic drugs in the clinical group); history of severe head injury; frequent alcohol consumption (several times per week); and use of other psychoactive substances. For the clinical group, additional exclusion criteria included having more than one epileptic focus and having undergone surgical treatment for epilepsy. Because of the small number of patients with right-hemisphere epileptic foci, which was insufficient for robust analysis, we chose to conduct analyses exclusively on patients with a left-sided focus (left-MTLE). Further details are provided in Table 1.

TABLE 1 Demographic and clinical characteristics of patients with left-MTLE and controls.

| | Left-MTLE group | Control group |
|--|-----------------|---------------|
| N | 21 | 28 |
| Age (years) | 39.71 (10.2) | 35.71 (10.7) |
| Years of education | 14.38 (2.7) | 14.21 (2.3) |
| Epilepsy duration (years) | 21.42 (8.8) | n/a |
| Age at epilepsy onset | 17.62 (13.3) | n/a |
| Frequency of focal seizures (monthly) | 14.29 (24.2) | n/a |
| Frequency of generalized seizures (annually) | 4.14 (9.8) | n/a |

Data presented as mean (SD); n/a, not applicable.

2.2 Procedure

All participants were examined individually over two separate sessions. The first session involved providing general information about the study and obtaining written informed consent, followed by a brief interview to collect demographic information and a neuropsychological assessment focused on evaluating memory functions. Patients with MTLE were also asked to provide information about their seizures and medical history. This session lasted approximately 60–90 min, varying between participants depending on their condition. The examination took place in a quiet, isolated, and well-lit room at the hospital. The second session involved MRI scanning, which all participants underwent. This part lasted approximately 1 h. All procedures were conducted in accordance with the Declaration of Helsinki and were approved by the Ethics Committee of the Faculty of Psychology at the University of Warsaw. All participants provided informed consent and received financial compensation for their participation.

2.3 Neuropsychological examination

To thoroughly assess participants' memory function, the Fourth Edition of the Wechsler Memory Scale (WMS-IV) was administered. The WMS-IV is a battery designed to evaluate various aspects of memory and working memory in adults. It assesses auditory memory, visual memory, visual working memory, immediate memory, and delayed memory. The WMS-IV includes seven subtests, four of which contain both immediate and delayed recall components (Wechsler, 2009).

2.3.1 Visual reproduction I

This subtest assesses non-verbal visual memory. The examiner presents a series of five designs, shown one at a time in a booklet for 10 s each. After viewing each design, the examinee is asked to draw it from memory as accurately as possible. There is no time limit for the drawing task.

2.3.2 Visual reproduction II

This subtest is administered 20–30 min after VR I and assesses long-term visuospatial memory. In the delayed condition, the examinee is asked to recall and draw from memory the designs they previously drew, in any order. After completing the free recall portion, the recognition task is administered. The examiner presents six different designs for each of the five original items, and the examinee must identify which design matches the one they were asked to remember in the VR I task.

2.3.3 Logical memory I

This subtest assesses narrative memory under free recall conditions. The examiner orally presents two short stories, one at a time. Immediately after each presentation, the examinee is asked to repeat the story, including as many details as they can recall.

2.3.4 Logical memory II

This subtest is administered 20–30 min after LM I and assesses long-term narrative memory through both free recall and recognition tasks. The examinee is asked to recall both stories

presented in the first part (LM I). After completing the free recall, the recognition portion is administered, during which the examinee answers 15 yes/no questions about each story.

2.3.5 Spatial addition

This subtest assesses visuospatial working memory through a visual addition task. The examinee is shown two 4×4 -cell grids from the Stimulus Booklet, each containing blue and red dots, presented one after the other for 5 s each. The examinee is instructed to remember the placement of the blue dots on each grid and to ignore the red dots. After viewing both grids, the examinee's task is to place blue and white dots on a Memory Grid according to a specific set of rules: blue dots should be placed in the same positions as those shown across both grids; white dots should be placed only where blue dots appeared in the same location on both grids. The examinee is also provided with red dots, which should not be placed on the grid. The test is discontinued after three consecutive incorrect responses.

2.3.6 Verbal paired associates I

This subtest assesses verbal memory based on associative learning. The examiner reads 14 word pairs (e.g., sky–cloud), then reads the first word of each pair, and the examinee is asked to provide the corresponding word. Each response must be given within 5 s. There are four trials using the same list of word pairs, but presented in a different order each time. If the examinee gives an incorrect response, the correct answer is provided.

2.3.7 Verbal paired associates II

This subtest is administered 20–30 min after VPA I and assesses long-term recall of verbally paired information. The examinee is presented with the first word of each of the 14 word pairs learned in VPA I and asked to recall the corresponding second word. In this condition, the word pairs are not read aloud by the examiner, and no cues are provided. The examinee has 10 s to respond to each item. Following the free recall portion, the recognition task is administered. In this task, the examinee is shown 40 word pairs and must identify whether each pair was part of the original list from the immediate condition, responding with yes or no.

2.3.8 Designs I

This subtest assesses spatial memory for visual material. The examiner presents a 4×4 -cell grid containing 4–8 designs (depending on the condition) for 10 s, then removes it from the examinee's view. The examinee must then select the designs from a set of 8 to 16 cards (also depending on the condition) and place them on a Memory Grid in the same locations as originally shown. The task includes four conditions of increasing difficulty: the first with four designs to remember, the second and third with six designs, and the fourth with eight designs.

2.3.9 Designs II

This subtest is administered 20–30 min after DE I and assesses long-term spatial and visual memory through free recall and recognition tasks. The examinee is asked to select cards from the immediate condition and place them on the Memory Grid in the same positions as before. Following the free recall task, the

examiner presents a series of grids containing various designs and asks the examinee to identify the two designs that match both the shape and placement from the immediate condition (DE I).

2.3.10 Symbol span

This subtest assesses visual working memory using novel visual stimuli. The examiner presents a series of abstract symbols on a page for 5 s. Then, a new page is shown with various symbols, and the examinee is asked to identify the symbols from the previous page and select them in the same order in which they were originally presented in the stimulus booklet. The number of symbols increases gradually throughout the task.

2.3.11 Additional memory indicators

To assess memory retention, an additional indicator was calculated: the sum of points scored in each subtest examining long-term memory (LM II, VPA II, VR II, DE II) was divided by the sum of points obtained in the corresponding immediate recall subtests (LM I, VPA I, VR I, DE I) and multiplied by 100. This yielded a percentage representing the proportion of stored information.

2.4 Neuroimaging data acquisition

MRI scans were performed using a 3.0 Tesla Skyra (Siemens) MRI scanner with a 16-channel head coil at the Department of Radiology, Medical University of Warsaw. All participants were scanned after completing the neuropsychological assessment. A three-dimensional brain volume imaging (3D-BRAVO) sequence was used to acquire structural images with the following parameters: repetition time (TR) = 2,200 ms, echo time (TE) = 4.94 ms, inversion time (TI) = 1,100 ms, flip angle (FA) = 7°, matrix size = 256 × 256, voxel size = 1 × 1 × 1 mm³, and 176 slices. A three-dimensional fluid-attenuated inversion recovery sequence was also performed with the following parameters: TR = 5,000 ms, TE = 371 ms, FA = 120°, matrix size = 256 × 256, voxel size = 1 × 1 × 1 mm³, and 176 slices.

2.5 Anatomical data processing

Raw T1-weighted DICOM images were reviewed and converted to NIfTI format using MRICron's dcm2niix (Li et al., 2016). Standard volumetric and surface processing pipelines were then implemented in FreeSurfer (version 7.2.0), as described in detail in the authors' original papers (see: Dale and Sereno, 1993; Dale et al., 1999; Fischl et al., 1999; Fischl and Dale, 2000). Briefly, the procedures included skull stripping, B1-bias field correction, and gray-white matter segmentation, followed by non-linear registration of individual images to stereotaxic atlases, which provided labels for brain regions. The standard FreeSurfer atlas was used for volumetric estimation of subcortical structures (Fischl et al., 2002), and the Desikan–Killiany anatomical atlas was used for cortical surface measurements (Desikan et al., 2006). Each patient's data underwent additional visual inspection to confirm the accuracy of the anatomical labeling. All volumetric measures were adjusted for individual estimated

intracranial volume to account for inter-subject differences in brain size.

2.6 Statistical analysis

Statistical analyses were conducted using IBM SPSS Statistics for Windows, version 29.0.2 (IBM Corp., Armonk, NY, United States). The Shapiro–Wilk test confirmed that the data followed a normal distribution, and other assumptions for parametric testing were also met. The independent-samples Student's *t*-test was used to compare mean scores between patients and healthy controls. Pearson's *r* coefficient was used to analyze correlations between continuous variables. To reduce the risk of false positives, a Bayesian local false discovery rate (FDR) correction was applied (threshold < 0.2), and significant results were obtained for each type of memory.

3 Results

3.1 Participant characteristics

Descriptive statistics for both groups are presented in Table 1. There were no significant differences in age ($t = -1.320$, $p = 0.097$) or years of education ($t = -0.232$, $p = 0.409$), allowing us to assume that any differences observed in neuropsychological test performance or gray matter volumetric properties were attributable to group effects rather than demographic differences.

3.2 Comparison of memory indicators in patients with MTLE and healthy controls

Intergroup comparisons revealed significant differences across most WMS indicators, with large or very large effect sizes in the majority of cases (Table 2).

The results obtained from the WMS-IV performance by the left-MTLE group and the control group are shown in Figure 1.

3.3 Comparison of structural gray matter measures in patients with left-MTLE and healthy controls

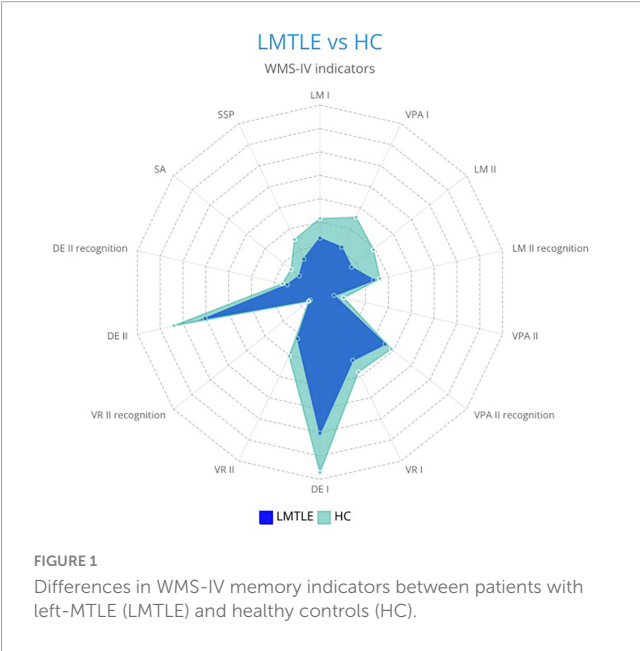
Statistically significant differences were found in intergroup comparisons between healthy controls and patients with left-MTLE in the following gray matter regions:

- Left hemisphere: cuneus ($t = 2.397$, $p = 0.010$), lateral occipital cortex ($t = 3.233$, $p = 0.001$), superior temporal gyrus ($t = -1.810$, $p = 0.040$), temporal pole ($t = -2.397$, $p = 0.010$), and hippocampus ($t = -1.926$, $p = 0.032$).
- Right hemisphere: caudal anterior cingulate gyrus ($t = 1.890$, $p = 0.032$), pars orbitalis ($t = -2.038$, $p = 0.024$), posterior cingulate gyrus ($t = 2.071$, $p = 0.022$), caudate nucleus ($t = 1.726$, $p = 0.045$), pallidum ($t = -1.893$, $p = 0.032$), and amygdala ($t = 1.701$, $p = 0.048$).

TABLE 2 Between-group comparisons of WMS-IV indicators.

| WMS-IV subtest | left-MTLE N = 21 M (SD) | HC N = 28 M (SD) | t | p | Cohen's d |
|--------------------|-------------------------------|------------------------|-------|---------|--------------|
| LM I | 23.10 (7.80) | 31.50 (7.32) | −3.87 | < 0.001 | −1.12 |
| LM II | 17.19 (7.96) | 29.18 (7.28) | −5.48 | < 0.001 | −1.58 |
| LM II recognition | 23.48 (3.49) | 26.21 (3.20) | −2.85 | 0.003 | −0.82 |
| % LM | 71.91 (22.07) | 93.83 (10.63) | −4.05 | < 0.001 | −1.28 |
| VPA I | 21.33 (8.45) | 35.54 (10.86) | −4.97 | < 0.001 | −1.43 |
| VPA II | 6.14 (3.20) | 10.38 (2.77) | −4.94 | < 0.001 | −1.43 |
| VPA II recognition | 35.52 (2.52) | 38.86 (1.21) | −6.13 | < 0.001 | −1.77 |
| % VPA | 83.83 (20.91) | 92.55 (13.32) | −1.78 | 0.041 | −0.51 |
| VR I | 32.24 (6.24) | 37.79 (3.77) | −3.61 | < 0.001 | −1.12 |
| VR II | 22.00 (7.94) | 30.29 (8.47) | −3.48 | < 0.001 | −1.00 |
| VR II recognition | 5.33 (1.28) | 6.14 (1.11) | −2.37 | 0.011 | −0.68 |
| % VR | 67.68 (19.99) | 79.53 (18.41) | −2.15 | 0.018 | −0.62 |
| DE I | 60.19 (13.08) | 76.96 (16.48) | −3.84 | < 0.001 | −1.11 |
| DE II | 50.29 (11.79) | 63.96 (18.12) | −3.01 | 0.002 | −0.87 |
| DE II recognition | 14.35 (2.11) | 16.46 (3.23) | −2.74 | 0.004 | −0.75 |
| % DE | 84.62 (17.29) | 82.95 (12.67) | 0.39 | 0.349 | 1.11 |
| SA | 11.24 (3.94) | 15.75 (3.60) | −4.17 | < 0.001 | −1.21 |
| SSP | 15.76 (4.72) | 25.00 (7.35) | −5.34 | < 0.001 | −1.45 |

Data presented as mean (SD). Statistically significant results are shown in bold. DE, designs; LM, logical memory; SD, standard deviation; SA, spatial addition; SSP, symbol span; VPA, verbal paired associates; VR, visual reproduction.



Bilateral differences were also observed in the cerebellar cortex: left cerebellum cortex ($t = -1.763, p = 0.042$) and right cerebellum cortex ($t = -2.158, p = 0.018$). Regions that were significantly smaller in patients with left-MTLE compared with healthy subjects included the left superior temporal gyrus, left temporal pole, left hippocampus, right pars

orbitalis, right pallidum, and bilateral cerebellum cortex. By contrast, regions that were significantly larger in patients with left-MTLE included the left cuneus, left lateral occipital cortex, right caudal anterior cingulate gyrus, right posterior cingulate gyrus, right caudate nucleus, and right amygdala.

3.4 Gray matter areas associated with memory performance in left-MTLE population

Correlation analyses were conducted within the left-MTLE group to explore the relationships between memory test performance and gray matter abnormalities. To enhance interpretability, WMS-IV subtests were grouped according to the specific type of memory they assessed:

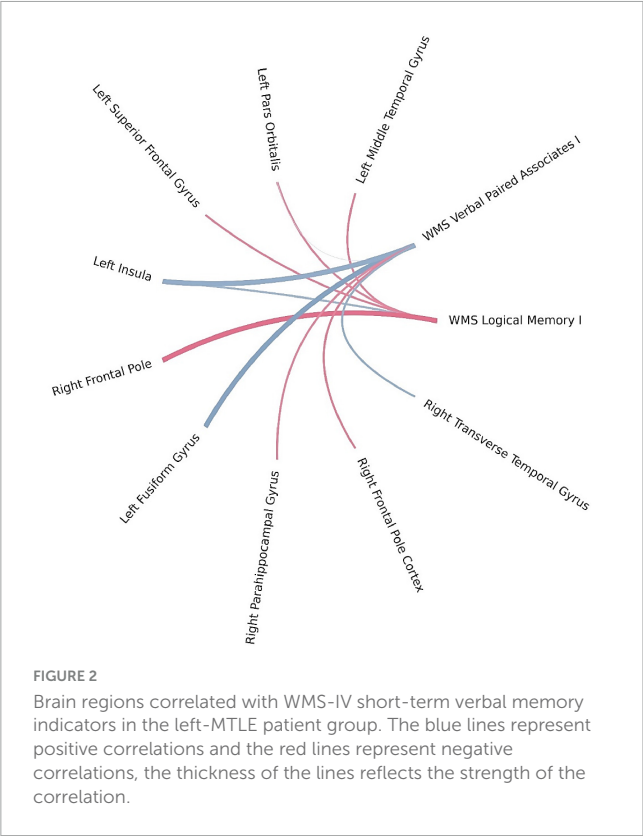
- Short-term verbal memory: LM I and VPA I
- Short-term visual memory: VR I and DE I
- Long-term verbal memory: LM II, LM II recognition,% LM, VPA II, VPA II recognition, and% VPA
- Long-term visual memory: VR II, VR II recognition,% VR, DE II, DE II recognition, and% DE
- Working memory: SA and SSP

Using Bayesian local FDR correction (threshold < 0.2), significant correlations were identified between short-term verbal memory performance and cortical thickness (see Table 3; Figure 2). Specifically, in patients with left-MTLE, short-term verbal memory scores were associated with cortical thickness in the following regions: the fusiform gyrus, insula, middle temporal gyrus, pars orbitalis, and superior frontal gyrus in the left hemisphere, and the frontal pole, parahippocampal gyrus, and transverse temporal gyrus in the right hemisphere.

TABLE 3 Gray matter areas associated with short-term verbal memory.

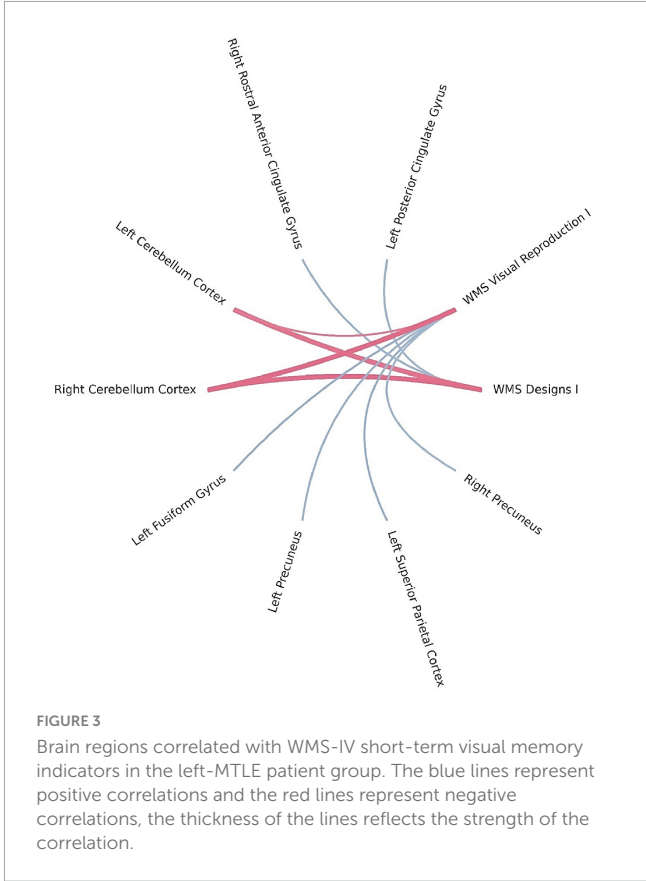
| Subtest | Brain region | r | p | Local FDR |
|-----------|------------------------------|--------|----------|-----------|
| WMS LM I | LH middle temporal gyrus | −0.468 | 0.032509 | 0.033591 |
| | LH pars orbitalis | −0.457 | 0.037217 | 0.040917 |
| | LH superior frontal gyrus | −0.472 | 0.030723 | 0.031697 |
| | LH insula | 0.448 | 0.04164 | 0.051126 |
| | RH frontal pole | −0.552 | 0.009531 | 0.058838 |
| WMS VPA I | LH pars orbitalis | 0.0524 | 0.82159 | 0.139467 |
| | LH fusiform gyrus | 0.583 | 0.00554 | 0.004859 |
| | LH insula | 0.521 | 0.015473 | 0.042904 |
| | RH parahippocampal gyrus | −0.454 | 0.038505 | 0.043539 |
| | RH frontal pole cortex | −0.484 | 0.026212 | 0.029118 |
| | RH transverse temporal gyrus | 0.49 | 0.024089 | 0.029132 |

RH, right hemisphere; LH, left hemisphere; LM, logical memory; VPA, verbal paired associates.



Bayesian local FDR analysis (threshold < 0.2) revealed significant correlations between short-term visual memory scores and brain structural measures (Table 4; Figure 3). Short-term visual memory was associated with the following regions: fusiform gyrus, precuneus, superior parietal cortex, and posterior cingulate gyrus in the left hemisphere; precuneus and rostral anterior cingulate gyrus in the right hemisphere; and the cerebellar cortex bilaterally.

Using Bayesian local FDR correction (threshold < 0.2), we identified significant correlations between long-term verbal



memory performance and cortical or subcortical brain structures. Detailed results are presented in Table 5 and Figure 4. Long-term verbal memory indicators were associated with the following regions: fusiform gyrus, isthmus cingulate gyrus, lateral occipital cortex, transverse temporal gyrus, insula, paracentral cortex, precentral gyrus, superior frontal gyrus, middle temporal gyrus, thalamus, pallidum, and hippocampus in the left hemisphere, and the transverse temporal gyrus, pericalcarine cortex, superior frontal gyrus, frontal pole, thalamus, and hippocampus in the right hemisphere.

As shown in Table 6 and Figure 5, the application of Bayesian local FDR correction (threshold < 0.2) revealed several significant associations between long-term visual memory performance and structural brain measures. The following regions were correlated with long-term visual memory indicators: caudal middle frontal gyrus, lateral orbitofrontal cortex, middle temporal gyrus, precuneus, rostral anterior cingulate gyrus, rostral middle frontal gyrus, inferior parietal cortex, superior parietal cortex, parahippocampal gyrus, paracentral cortex, pars triangularis, pericalcarine cortex, superior frontal gyrus, insula, cuneus, pallidum, and amygdala in the left hemisphere, and caudal middle frontal gyrus, rostral middle frontal gyrus, posterior cingulate gyrus, frontal pole, superior frontal gyrus, paracentral cortex, thalamus, and pallidum in the right hemisphere, along with the cerebellar cortex bilaterally.

Bayesian local FDR correction (threshold < 0.2) identified significant correlations between working memory performance and structural brain features (Table 7). The following regions were associated with working memory indicators: the superior parietal

TABLE 4 Gray matter areas associated with short-term visual memory.

| Subtest | Brain region | <i>r</i> | <i>p</i> | Local FDR |
|----------|-------------------------------------|----------|----------|-----------|
| WMS DE I | LH posterior cingulate gyrus | 0.443 | 0.044285 | 0.06088 |
| | RH rostral anterior cingulate gyrus | 0.455 | 0.038292 | 0.04592 |
| | Left cerebellum cortex | −0.539 | 0.011617 | 0.078387 |
| | Right cerebellum cortex | −0.56 | 0.008286 | 0.007663 |
| WMS VR I | LH fusiform gyrus | 0.486 | 0.025432 | 0.039662 |
| | LH precuneus cortex | 0.454 | 0.03881 | 0.04692 |
| | LH superior parietal cortex | 0.474 | 0.029764 | 0.037265 |
| | RH precuneus cortex | 0.439 | 0.046413 | 0.068079 |
| | Left cerebellum cortex | −0.5 | 0.021014 | 0.050482 |
| | Right cerebellum cortex | −0.567 | 0.007292 | 0.001009 |

RH, right hemisphere; LH, left hemisphere; DE, designs; VR, visual reproduction.

TABLE 5 Gray matter areas associated with long-term verbal memory.

| Subtest | Brain region | <i>R</i> | <i>p</i> | Local FDR |
|------------------------|------------------------------|----------|----------|-----------|
| WMS LM II | LH paracentral cortex | −0.449 | 0.041342 | 0.177075 |
| | LH superior frontal gyrus | −0.481 | 0.02729 | 0.117357 |
| | RH superior frontal gyrus | −0.444 | 0.043907 | 0.188958 |
| | RH frontal pole cortex | −0.545 | 0.010537 | 0.087175 |
| WMS LM II recognition | LH paracentral cortex | −0.559 | 0.008389 | 0.08935 |
| | LH precentral gyrus | −0.448 | 0.041608 | 0.178303 |
| | RH frontal pole | −0.51 | 0.018081 | 0.091004 |
| % LM | LH paracentral cortex | −0.49 | 0.024158 | 0.106654 |
| | RH pericalcarine cortex | 0.545 | 0.010703 | 0.087016 |
| WMS VPA II | LH fusiform gyrus | 0.599 | 0.004124 | 0.048965 |
| | LH lateral occipital cortex | 0.5 | 0.021033 | 0.097607 |
| | RH frontal pole | −0.487 | 0.025024 | 0.109467 |
| | RH transverse temporal gyrus | 0.476 | 0.029093 | 0.124114 |
| WMS VPA II recognition | LH isthmus cingulate gyrus | 0.487 | 0.025269 | 0.110284 |
| | LH transverse temporal gyrus | 0.523 | 0.014996 | 0.086778 |
| | LH insula | 0.524 | 0.014812 | 0.086631 |
| | RH transverse temporal gyrus | 0.499 | 0.021349 | 0.098435 |
| | Right hippocampus | 0.466 | 0.033208 | 0.140799 |
| % VPA | LH middle temporal gyrus | −0.455 | 0.038139 | 0.16244 |
| | Left thalamus | −0.503 | 0.020128 | 0.095358 |
| | Left Pallidum | −0.608 | 0.003446 | 0.027508 |
| | Left hippocampus | −0.474 | 0.029838 | 0.127014 |
| | Right thalamus | −0.573 | 0.006567 | 0.087041 |

RH, right hemisphere; LH, left hemisphere; LM, logical memory; VPA, verbal paired associates.

cortex in the left hemisphere, the cuneus and posterior cingulate gyrus in the right hemisphere, and the cerebellar cortex bilaterally (Figure 6).

3.5 Association between gray matter volume, memory performance, and clinical variables in left-MTLE population

No significant correlations were found between age at epilepsy onset and any memory indicators. However, epilepsy duration was significantly correlated with two long-term visual memory measures: VR II ($r = -0.539$, $p = 0.012$) and % VR ($r = -0.491$, $p = 0.024$).

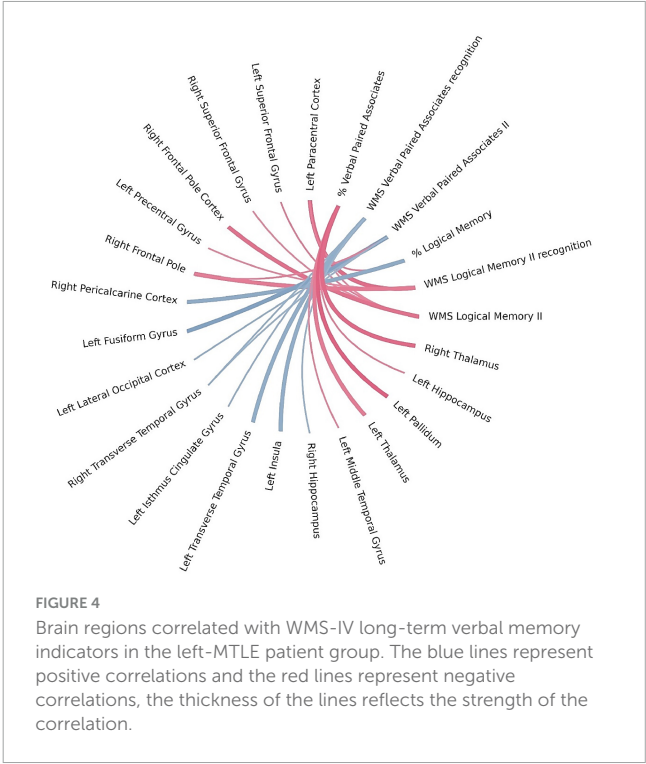


FIGURE 4 Brain regions correlated with WMS-IV long-term verbal memory indicators in the left-MTLE patient group. The blue lines represent positive correlations and the red lines represent negative correlations, the thickness of the lines reflects the strength of the correlation.

By contrast, age at epilepsy onset showed significant negative correlations with gray matter volume in several regions: left inferior temporal cortex ($r = -0.514$, $p = 0.017$), left isthmus cingulate gyrus ($r = -0.446$, $p = 0.043$), left middle temporal gyrus ($r = -0.464$, $p = 0.034$), left thalamus ($r = -0.434$, $p = 0.049$), left pallidum ($r = -0.497$, $p = 0.022$), left hippocampus ($r = -0.518$, $p = 0.016$), right superior frontal gyrus ($r = -0.449$, $p = 0.041$), and right pallidum ($r = -0.469$, $p = 0.032$).

These findings suggest that a longer duration of epilepsy is associated with more severe long-term visual memory deficits, while an older age at epilepsy onset is linked to greater gray matter volume reduction in the specified regions.

4 Discussion

This study combined morphometric MRI techniques with neuropsychological testing to assess changes in the functional and structural organization associated with MTLE. The findings clearly show that patients with MTLE exhibit significantly reduced memory functioning, consistent with previous studies on this population (Rayner et al., 2016; Zhu et al., 2021; Novak et al., 2022).

In analyzing gray matter abnormalities, we found that patients with left-MTLE showed significant alterations in the volumes of specific brain regions. These changes were observed not only near the epileptic focus but also in more distant brain areas. Notably, volume reductions were found in the temporal lobe (superior temporal gyrus and temporal pole) and in more remote regions, such as the right frontal lobe (pars orbitalis) and the right globus pallidus. A decrease in gray matter volume was also observed bilaterally in the cerebellar cortex—findings consistent with previous research (Colnaghi et al., 2017; Zhang et al., 2017). Although other studies have reported bilateral thalamic volume

TABLE 6 Gray matter areas associated with long-term visual memory.

| Subtest | Brain region | <i>r</i> | <i>p</i> | Local FDR |
|-----------------------|-------------------------------------|----------|----------|-----------|
| WMS DE II | LH parahippocampal gyrus | 0.456 | 0.037749 | 0.113731 |
| | LH pericalcarine cortex | −0.507 | 0.019022 | 0.121909 |
| WMS DE II recognition | LH caudal middle frontal gyrus | −0.475 | 0.034313 | 0.105051 |
| | LH inferior parietal cortex | −0.491 | 0.02788 | 0.096946 |
| | LH paracentral cortex | −0.528 | 0.016818 | 0.145071 |
| | LH superior parietal cortex | −0.478 | 0.032931 | 0.10231 |
| | RH paracentral cortex | −0.524 | 0.017816 | 0.133018 |
| | Left Amygdala | 0.459 | 0.041583 | 0.126123 |
| | Right Thalamus | 0.445 | 0.049561 | 0.159349 |
| | LH cuneus | −0.447 | 0.04243 | 0.129203 |
| | LH pars triangularis | −0.444 | 0.043726 | 0.134135 |
| % DE | Left pallidum | 0.508 | 0.018715 | 0.124431 |
| | Right pallidum | 0.453 | 0.039092 | 0.11777 |
| | LH lateral orbitofrontal cortex | 0.471 | 0.031157 | 0.09952 |
| | LH middle temporal gyrus | −0.444 | 0.043747 | 0.134217 |
| WMS VR II | LH insula | 0.475 | 0.029506 | 0.097759 |
| | Right cerebellum cortex | −0.467 | 0.032872 | 0.102204 |
| | RH banks STS | −0.467 | 0.032604 | 0.101732 |
| | RH posterior cingulate gyrus | −0.452 | 0.039741 | 0.119842 |
| WMS VR II recognition | RH frontal pole | −0.456 | 0.037782 | 0.113826 |
| | Left cerebellum cortex | −0.461 | 0.035358 | 0.107422 |
| | Right cerebellum cortex | −0.48 | 0.027771 | 0.096928 |
| | LH paracentral cortex | −0.462 | 0.034783 | 0.106087 |
| % VR | LH precuneus | −0.452 | 0.039663 | 0.119589 |
| | LH rostral anterior cingulate gyrus | −0.48 | 0.027756 | 0.096926 |
| | LH rostral middle frontal gyrus | −0.602 | 0.003886 | 0.031644 |
| | LH insula | 0.466 | 0.033169 | 0.102749 |
| | RH caudal middle frontal gyrus | −0.464 | 0.033966 | 0.104319 |
| | RH rostral middle frontal gyrus | −0.468 | 0.032559 | 0.101654 |
| | RH superior frontal gyrus | −0.48 | 0.027495 | 0.096906 |
| | | | | |

RH, right hemisphere; LH, left hemisphere; DE, designs; VR, visual reproduction.

reductions in patients with MTLE (Wei et al., 2016; Zheng et al., 2018), this was not observed in the present study.

In addition, compared with healthy participants, patients with left-MTLE showed increased volume in the cuneus and

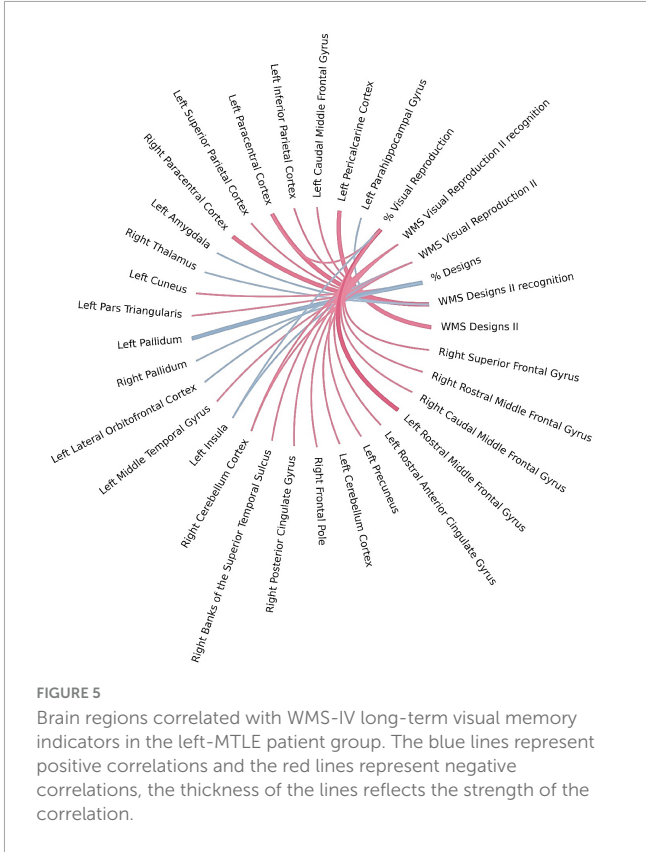


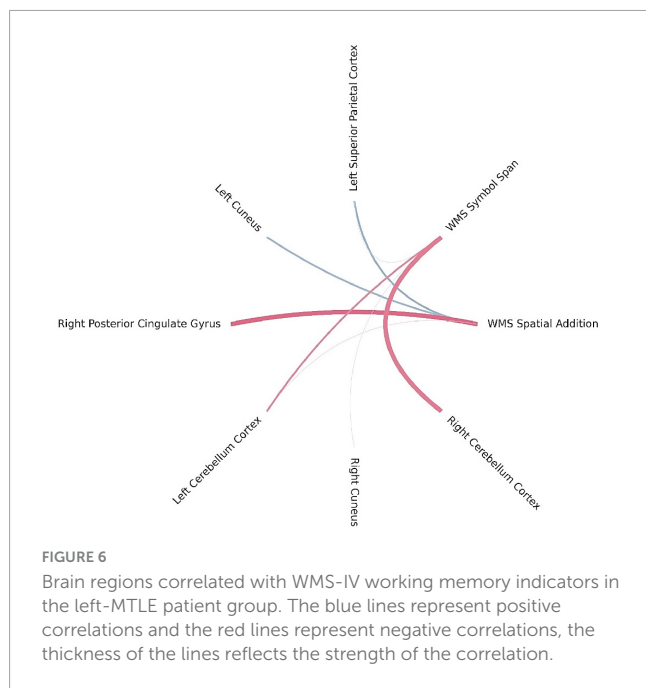
FIGURE 5 Brain regions correlated with WMS-IV long-term visual memory indicators in the left-MTLE patient group. The blue lines represent positive correlations and the red lines represent negative correlations, the thickness of the lines reflects the strength of the correlation.

TABLE 7 Gray matter areas associated with working memory.

| Subtest | Brain region | <i>r</i> | <i>p</i> | Local FDR |
|---------|-------------------------------|----------|----------|-----------|
| WMS SA | LH superior parietal cortex | 0.493 | 0.023092 | 0.035573 |
| | LH cuneus | 0.442 | 0.04492 | 0.112121 |
| | RH posterior cingulate cortex | −0.583 | 0.005516 | 0.001799 |
| | Left cerebellum cortex | −0.0668 | 0.773722 | 0.006785 |
| WMS SSP | LH superior parietal cortex | 0.0778 | 0.737522 | 0.140889 |
| | RH cuneus | 0.0775 | 0.738595 | 0.131409 |
| | Left cerebellum cortex | −0.455 | 0.038251 | 0.056754 |
| | Right cerebellum cortex | −0.509 | 0.018502 | 0.052504 |

RH, right hemisphere; LH, left hemisphere; SA, spatial addition; SSP, symbol span.

the lateral part of the occipital lobe in the left hemisphere (the side of the epileptic focus), as well as in the caudal anterior cingulate cortex, posterior cingulate cortex, caudate nucleus, and amygdala in the right hemisphere (contralateral to the epileptic focus). As demonstrated in the study by Zubal et al. (2025), this hypertrophy—particularly in the contralateral amygdala—may result from the negative impact of seizures and the brain’s compensatory response to cognitive deficits. Other studies have also reported amygdala enlargement in temporal lobe epilepsy. While some of these focused on the amygdala ipsilateral to the epileptic focus (Kim et al., 2012; Mitsueda-Ono et al., 2011; Bower et al., 2003), three studies have documented enlargement in the



contralateral amygdala (Coan et al., 2013; Whelan et al., 2018; Zubal et al., 2025). However, only one of these (Zubal et al., 2025) linked this finding to memory impairment.

Although we did not find a correlation between contralateral amygdala volume and memory performance, as reported by Zubal et al. (2025), it is possible that the hypertrophy observed in other regions—both ipsilateral and contralateral to the epileptic focus—may have arisen through a similar compensatory mechanism. In light of this, the detection of negative correlations between memory function and the volume of certain brain regions is particularly noteworthy.

For the WMS LM I task, significant negative correlations were observed with the left middle temporal gyrus, superior frontal gyrus, pars orbitalis, and right frontal pole, suggesting that reduced cortical thickness in these regions may be associated with better immediate verbal memory recall. Interestingly, a positive correlation was also found with the left insula, indicating potential region-specific contributions to encoding or attentional control. The WMS VPA I task showed positive correlations with the left fusiform gyrus, left insula, and right transverse temporal gyrus—regions well known for their involvement in auditory-verbal processing (Liegeois-Chauvel et al., 1991; Skipper and Small, 2006; Price, 2010). By contrast, negative correlations were observed with the right frontal pole and parahippocampal cortex. These findings are not entirely consistent with other studies, which report that the ability to temporarily maintain speech-related information is associated with the left insula as well as other regions in the dominant hemisphere, such as the inferior frontal premotor regions, parietal cortex, and Broca's area (Vallar, 2006; Cascella and Al Khalili, 2024)—components of the language system that are clearly linked to the verbal modality of the task (Liegeois-Chauvel et al., 1991; Skipper and Small, 2006; Price, 2010). Additionally, research by Ćurčić-Blake et al. (2017) highlights that inhibitory deficits could contribute to failures in controlling the contents of memory and that the putamen is involved in translating memories

into language experience—findings consistent with our results, which suggest a complex interplay between fronto-limbic and temporal regions during associative verbal learning. For short-term visual memory, positive correlations were observed with the posterior cingulate gyrus, rostral anterior cingulate gyrus, fusiform gyrus, precuneus, and superior parietal cortex, underscoring the role of visuospatial integration, object recognition, and attention control in short-term visual reproduction. Additionally, negative correlations were found between WMS DE I and WMS VR I scores and the volume of the left and right cerebellar cortex, which may reflect reduced reliance on subcortical motor planning during efficient visual encoding. Our findings are consistent with studies on the neuronal correlates of visual short-term memory, which highlight the involvement of the occipital extrastriate cortex, posterior parietal cortex, prefrontal cortex, dorsal frontal area, parietal lobule, frontal premotor regions, and insula (Zimmer, 2008; Cascella and Al Khalili, 2024). Interestingly, our study found correlations between short-term memory and the insula only in the verbal modality. The association with the cerebellar cortex may be explained by the simultaneous involvement of working memory, which could be due to the complexity of the neuropsychological tasks.

The structure most commonly emphasized in long-term declarative memory is the hippocampus, where the consolidation of information from short-term to long-term memory takes place (Almaraz-Espinoza and Grider, 2023). The amygdala, by contrast, is associated with the emotional aspects of remembered information, which are further stored throughout the cortex (Almaraz-Espinoza and Grider, 2023). Some studies also highlight the role of prefrontal regions in memory recall (Braver et al., 2001). The results obtained in the present research are consistent with these findings, particularly in the domain of visual long-term memory: significant correlations were observed with prefrontal executive regions, temporo-parietal regions, the insula, pallidum, and amygdala in the left hemisphere, as well as the thalamus and pallidum in the right hemisphere.

It should be noted that we found positive correlations primarily in the hemisphere ipsilateral to the epileptic focus. In terms of long-term verbal memory, the results included both positive and negative correlations across a range of cortical and subcortical regions. Notably, lower scores on the % VPA task were associated with reduced volumes in the left and right thalamus, left pallidum, and left hippocampus, suggesting a potential role for subcortical memory circuits in verbal learning (O'Mara and Aggleton, 2019). Positive associations were observed between WMS VPA II recognition and cortical thickness in regions such as the insula, transverse temporal gyrus, and cingulate isthmus, while WMS VPA II showed both positive and negative correlations with occipital, temporal, and notably frontal areas—structures more commonly linked to short-term memory (Nee et al., 2013; Eriksson et al., 2015). Performance on WMS LM II and WMS LM II recognition was negatively correlated with thickness in the frontal pole, superior frontal gyrus, paracentral, and precentral regions, suggesting inefficiency of frontal-executive structures in narrative memory retrieval (Meléndez et al., 2019). Additionally, % LM scores were associated with cortical thickness in both the occipital and paracentral cortices, emphasizing the role of fronto-temporo-limbic networks in long-term verbal memory. A particularly intriguing finding was the negative correlation between long-term

verbal memory and the left hippocampus, alongside a positive correlation with the right hippocampus in patients with left-MTLE. This may indicate that as the left hippocampus becomes smaller and less functional, the right hippocampus, through neuronal reorganization and plasticity, increasingly assumes its functions. As a result, enlargement of the right hippocampus in left-MTLE may reflect compensatory adaptation, and greater right hippocampal volume may correspond with better memory performance because it takes on the role of supporting verbal memory. A study by [Chen et al. \(2017\)](#), which used resting-state functional connectivity (RSFC), supports this interpretation. Their findings showed that in individuals with left-MTLE, enhanced interhemispheric RSFC between the left hippocampus/amygdala and the right hippocampus was associated with better verbal memory, while increased RSFC between the left hippocampus and the left postcentral gyrus was linked to poorer verbal memory performance.

It should also be noted that some studies suggest a thinner cerebral cortex may indicate more effective and efficient neuronal systems ([Menary et al., 2013](#); [Wagstyl and Lerch, 2018](#)). Thus, the results obtained in our study—showing a thinner cortex in patients with left-MTLE—can be interpreted in two distinct ways. A longitudinal study in patients with MTLE, collecting data on changes in various aspects of memory at different stages of the disease and taking into account neuroanatomical alterations, could help clarify which interpretation is more accurate.

For WMS SA, higher scores were positively associated with the left superior parietal and right cuneus cortical thickness and negatively with the right posterior cingulate cortex. These regions are classically involved in visuospatial integration and attentional regulation ([Leech and Sharp, 2014](#)), suggesting that efficient activation of parietal and cingulate regions supports spatial memory processing. The WMS SSP task showed similar involvement of parietal and occipital regions, with significant positive correlations in the left superior parietal and right cuneus and negative correlations with the left and right cerebellar cortex, suggesting a potential modulatory role of cerebellar–cortical networks in spatial working memory tasks. The left hemisphere superior parietal area and right hemisphere cuneus correlated positively with working memory, which is consistent with the study by [Eriksson et al. \(2015\)](#), who indicate that the superior parietal cortex is involved in the executive aspects of working memory and with working memory capacity. However, they indicated a strong connection not of the left, but of the right parietal cortex with the spatial working memory task, which is the one used in this study ([Eriksson et al., 2015](#)). Furthermore, we did not find a correlation with the prefrontal cortex, which is highlighted as critical in working memory, especially the dorsal PFC, as the one more strongly involved in spatial working memory task ([Ptak, 2012](#); [Nee et al., 2013](#); [Eriksson et al., 2015](#)). Although we did not find a correlation with the prefrontal cortex, our findings—along with those of other studies—support the idea that a network of frontal and parietal cortical areas, along with the cerebellum ([Brissenden and Somers, 2019](#)), collectively referred to as the dorsal attention network, supports visual attentional function ([Ptak, 2012](#)).

An interesting study was conducted by [Zhang et al. \(2017\)](#), who described the hippocampus-associated causal network of structural damage in temporal lobe epilepsy. In this study, the researchers examined gray matter changes in patients with MTLE,

depending on the duration of epilepsy and the estimated number of lifetime seizures. They introduced the term Granger Causality (GC), which measures the strength of effective connectivity—representing causal interactions by assessing how activity in one neural region influences another. It quantifies the extent to which the signal from a seed region can predict the signal in a target region ([Vanneste et al., 2021](#); [Granger, 1969](#)). The authors observed that the lateral temporal lobe ipsilateral to the epileptogenic focus, bilateral lateral prefrontal cortex, medial prefrontal cortex, insula, and thalamus showed consistently positive GC values, while the contralateral temporal cortex, posterior cingulate cortex, and amygdala showed consistently negative GC values. The bilateral basal ganglia, including the caudate head and putamen, were characterized by divergent GC values across different analyses.

A positive GC value indicates that the reduction in gray matter volume within a region is causally linked to, and follows, hippocampal atrophy—suggesting a potential seizure-related damaging effect originating from the hippocampus. By contrast, a negative GC value indicates that a region shows an opposing (increased) gray matter volume alteration in response to hippocampal atrophy, which is interpreted as a compensatory structural effect ([Zhang et al., 2017](#)). In our study, we observed a decrease in gray matter volume in the lateral temporal lobe ipsilateral to the epileptogenic focus, the contralateral prefrontal cortex, and the ipsilateral hippocampus—findings that likely reflect damage driven by hippocampal atrophy. Presumably, this degeneration contributes to increased cognitive deficits. Conversely, an observed increase in the contralateral posterior cingulate cortex and amygdala may represent a protective or compensatory response. This supports the idea of a complex repair mechanism in which less affected brain regions are recruited to support cognitive functioning. Further evidence of this process comes from the positive correlations we observed between memory indicators and the right hemisphere transverse temporal gyrus and pallidum, which may suggest that functional reorganization in these areas has already occurred. On the other hand, the negative correlation between memory indicators and the contralateral posterior cingulate cortex—despite its increased volume in patients with epilepsy—may indicate that while structural reorganization has taken place, functional reorganization in this region has yet to follow.

These findings emphasize the involvement of fronto-temporo-limbic networks in memory and support the utility of local FDR methods in uncovering subtle yet meaningful brain–behavior relationships that may be overlooked using more conservative correction procedures. Although none of these results survived classical FDR correction, the application of local FDR revealed potentially meaningful effects that would otherwise remain undetected. The findings underscore the role of frontal, temporal, and limbic structures in supporting different types of memory performance. Additionally, several subcortical regions—such as the thalamus, pallidum, and hippocampus—also emerged, suggesting the involvement of broader memory-related networks.

Although some studies have evaluated memory ([Butler and Zeman, 2008](#); [Baulac, 2015](#); [Rayner et al., 2016](#); [Zhu et al., 2021](#)) and brain abnormalities in patients with MTLE ([Bonilha et al., 2012](#); [Xie et al., 2024](#); [Ishizaki et al., 2025](#)), only a few have combined the two approaches ([Cabalo et al., 2024](#); [Park et al., 2017](#)). Furthermore, there is a scarcity of studies that collect such detailed data on the

various facets of memory in patients with epilepsy, which allow for a comprehensive examination of patients' memory profiles and their relationship to anatomical correlates. Our study attempts to address this gap.

5 Conclusion

This work enriches our understanding of the specificity of the memory system in patients with temporal lobe epilepsy. Patients performed worse than the control group, exhibiting a broad range of deficits across all assessed types and modalities of memory. Particularly noteworthy is the study's identification of a distinct pattern of neuronal aberrations and correlations between specific brain structures and memory performance. The use of Bayesian local FDR correction enabled the detection of meaningful structure–function relationships that may have gone unnoticed with more conservative correction methods. These findings suggest that the degree of structural brain anomalies may be linked to the extent of memory impairment in temporal lobe epilepsy, highlighting the complex interplay between neuroanatomy and cognitive function. Some results from this study support a tentative model: an initial structural reduction leads to cognitive difficulty, followed by structural reorganization, and eventually functional reorganization that may enable cognitive improvement. Therefore, even when increases in certain brain structures are observed—previously reported in other studies as potentially protective—this does not necessarily translate into improved cognitive outcomes. Further research is needed to clarify the mechanisms underlying these memory deficits. Given the limited sample size in the present study, replication and extension through longitudinal research would be valuable for observing structural and mnemonic changes over time. Such studies could help determine whether hypertrophy in specific structures results from bioelectrical abnormalities associated with seizures or reflects a plasticity-driven reorganization of brain networks aimed at mitigating memory or broader cognitive deficits.

Data availability statement

The raw data supporting the conclusions of this article will be made available by the authors, without undue reservation.

Ethics statement

The studies involving humans were approved by the Ethics Committee of the Faculty of Psychology at the University of

Warsaw. The studies were conducted in accordance with the local legislation and institutional requirements. The participants provided their written informed consent to participate in this study.

Author contributions

AO: Conceptualization, Data curation, Funding acquisition, Investigation, Methodology, Project administration, Resources, Visualization, Writing – original draft, Writing – review & editing. AB: Conceptualization, Data curation, Funding acquisition, Methodology, Project administration, Resources, Supervision, Writing – original draft, Writing – review & editing. WR: Data curation, Visualization, Writing – original draft. AR: Data curation, Writing – review & editing. MK-B: Data curation, Writing – review & editing. PN: Data curation, Software, Writing – original draft. PK: Writing – review & editing. AG-N: Data curation, Visualization, Writing – original draft.

Funding

The author(s) declare that financial support was received for the research and/or publication of this article. This work was supported by the University of Warsaw.

Conflict of interest

The authors declare that the research was conducted in the absence of any commercial or financial relationships that could be construed as a potential conflict of interest.

Generative AI statement

The authors declare that no Generative AI was used in the creation of this manuscript.

Publisher's note

All claims expressed in this article are solely those of the authors and do not necessarily represent those of their affiliated organizations, or those of the publisher, the editors and the reviewers. Any product that may be evaluated in this article, or claim that may be made by its manufacturer, is not guaranteed or endorsed by the publisher.

References

- Almaraz-Espinoza, A., and Grider, M. H. (2023). "Physiology, long term memory," in *StatPearls*. Treasure Island, FL: StatPearls Publishing.
- Bala, A., Olejnik, A., Mojżeszczak, M., Rysz, A., and Kunert, P. (2024). Navigating social waters: Understanding theory-of-mind challenges in patients with mesial temporal lobe epilepsy. *J. Clin. Med.* 13:1410. doi: 10.3390/jcm13051410
- Baulac, M. (2015). MTLE with hippocampal sclerosis in adult as a syndrome. *Revue Neurol.* 171, 259–266. doi: 10.1016/j.neurol.2015.02.004
- Bell, B. D., Seidenberg, M., Hermann, B. P., and Douville, K. (2003). Visual and auditory naming in patients with left or bilateral temporal lobe epilepsy. *Epilepsy Res.* 55, 29–37. doi: 10.1016/s0920-1211(03)00110-4

- Bonilha, L., Nesland, T., Martz, G. U., Joseph, J. E., Spampinato, M. V., Edwards, J. C., et al. (2012). Medial temporal lobe epilepsy is associated with neuronal fibre loss and paradoxical increase in structural connectivity of limbic structures. *J. Neurol. Neurosurg. Psychiatry* 83, 903–909. doi: 10.1136/jnnp-2012-302476
- Bower, S. P., Vogrin, S. J., Morris, K., Cox, I., Murphy, M., Kilpatrick, C. J., et al. (2003). Amygdala volumetry in “imaging-negative” temporal lobe epilepsy. *J. Neurol. Neurosurg. Psychiatry* 74, 1245–1249. doi: 10.1136/jnnp.74.9.1245
- Braver, T. S., Barch, D. M., Kelley, W. M., Buckner, R. L., Cohen, N. J., Miezin, F. M., et al. (2001). Direct comparison of prefrontal cortex regions engaged by working and long-term memory tasks. *NeuroImage* 14, 48–59. doi: 10.1006/nimg.2001.0791
- Brissenden, J. A., and Somers, D. C. (2019). Cortico-cerebellar networks for visual attention and working memory. *Curr. Opin. Psychol.* 29, 239–247. doi: 10.1016/j.copsyc.2019.05.003
- Butler, C. R., and Zeman, A. Z. (2008). Recent insights into the impairment of memory in epilepsy: Transient epileptic amnesia, accelerated long-term forgetting and remote memory impairment. *Brain J. Neurol.* 131, 2243–2263. doi: 10.1093/brain/awn127
- Cabalo, D. G., DeKraker, J., Royer, J., Xie, K., Tavakol, S., Rodríguez-Cruces, R., et al. (2024). Differential reorganization of episodic and semantic memory systems in epilepsy-related mesiotemporal pathology. *Brain J. Neurol.* 147, 3918–3932. doi: 10.1093/brain/awae197
- Caciagli, L., Paquola, C., He, X., Vollmar, C., Centeno, M., Wandschneider, B., et al. (2023). Disorganization of language and working memory systems in frontal versus temporal lobe epilepsy. *Brain J. Neurol.* 146, 935–953. doi: 10.1093/brain/awac150
- Casella, M., and Al Khalili, Y. (2024). “Short-term memory impairment,” in *StatPearls*. Treasure Island, FL: StatPearls Publishing.
- Chen, S., Adepu, M., Emady, H., Jiao, Y., and Gel, A. (2017). Enhancing the physical modeling capability of open-source MFIX-DEM software for handling particle size polydispersity: Implementation and validation. *Powder Technol.* 317:55. doi: 10.1016/j.powtec.2017.04.055
- Coan, A. C., Morita, M. E., Campos, B. M., Bergo, F. P., Kubota, B. Y., and Cendes, F. (2013). Amygdala enlargement occurs in patients with mesial temporal lobe epilepsy and hippocampal sclerosis with early epilepsy onset. *Epilepsy Behav.* 29, 390–394. doi: 10.1016/j.yebeh.2013.08.022
- Colnaghi, S., Beltrami, G., Poloni, G., Pichiecchio, A., Bastianello, S., Galimberti, C. A., et al. (2017). Parahippocampal involvement in mesial temporal lobe epilepsy with hippocampal sclerosis: A proof of concept from memory-guided saccades. *Front. Neurol.* 8:595. doi: 10.3389/fneur.2017.00595
- Ćurčić-Blake, B., Ford, J. M., Hubl, D., Orlov, N. D., Sommer, I. E., Waters, F., et al. (2017). Interaction of language, auditory and memory brain networks in auditory verbal hallucinations. *Progr. Neurobiol.* 148, 1–20. doi: 10.1016/j.pneurobio.2016.11.002
- Dale, A. M., and Sereno, M. I. (1993). Improved localization of cortical activity by combining EEG and MEG with MRI cortical surface reconstruction: A linear approach. *J. Cogn. Neurosci.* 5, 162–176. doi: 10.1162/jocn.1993.5.2.162
- Dale, A. M., Fischl, B., and Sereno, M. I. (1999). Cortical surface-based analysis. I. Segmentation and surface reconstruction. *NeuroImage* 9, 179–194. doi: 10.1006/nimg.1998.0395
- Desikan, R. S., Ségonne, F., Fischl, B., Quinn, B. T., Dickerson, B. C., Blacker, D., et al. (2006). An automated labeling system for subdividing the human cerebral cortex on MRI scans into gyral based regions of interest. *NeuroImage* 31, 968–980. doi: 10.1016/j.neuroimage.2006.01.021
- Dos Santos, Silva, R. P., Lima Angelo, I. C. B., De Medeiros Dantas, G. C., De Souza, J. M., Pinheiro Pessoa, J. R. C., et al. (2024). Pattern of abnormalities on gray matter in patients with mesial temporal lobe epilepsy and hippocampal sclerosis: An updated meta-analysis. *Clin. Neurol. Neurosurg.* 245:108473. doi: 10.1016/j.clineuro.2024.108473
- Eriksson, J., Vogel, E. K., Lansner, A., Bergström, F., and Nyberg, L. (2015). Neurocognitive architecture of working memory. *Neuron* 88, 33–46. doi: 10.1016/j.neuron.2015.09.020
- Fischl, B., and Dale, A. M. (2000). Measuring the thickness of the human cerebral cortex from magnetic resonance images. *Proc. Natl. Acad. Sci. U S A.* 97, 11050–11055. doi: 10.1073/pnas.200033797
- Fischl, B., Salat, D. H., Busa, E., Albert, M., Dieterich, M., Haselgrove, C., et al. (2002). Whole brain segmentation: Automated labeling of neuroanatomical structures in the human brain. *Neuron* 33, 341–355. doi: 10.1016/s0896-6273(02)00569-x
- Fischl, B., Sereno, M. I., and Dale, A. M. (1999). Cortical surface-based analysis. II: Inflation, flattening, and a surface-based coordinate system. *NeuroImage* 9, 195–207. doi: 10.1006/nimg.1998.0396
- Granger, C. W. J. (1969). Investigating causal relations by econometric models and cross-spectral methods. *Econometrica* 37, 424–438. doi: 10.2307/1912791
- Ishizaki, T., Maesawa, S., Suzuki, T., Hashida, M., Ito, Y., Yamamoto, H., et al. (2025). Frequency-specific network changes in mesial temporal lobe epilepsy: Analysis of chronic and transient dysfunctions in the temporo-amygdala-orbitofrontal network using magnetoencephalography. *Epilepsia Open* 10, 557–570. doi: 10.1002/epi4.70018
- Ives-Deliperi, V., and Butler, J. T. (2021). Mechanisms of cognitive impairment in temporal lobe epilepsy: A systematic review of resting-state functional connectivity studies. *Epilepsy Behav.* 115:107686. doi: 10.1016/j.yebeh.2020.107686
- Kim, D. W., Lee, S. K., Chung, C. K., Koh, Y. C., Choe, G., and Lim, S. D. (2012). Clinical features and pathological characteristics of amygdala enlargement in mesial temporal lobe epilepsy. *J. Clin. Neurosci.* 19, 509–512. doi: 10.1016/j.jocn.2011.05.042
- Kwan, P., and Sander, J. W. (2004). The natural history of epilepsy: An epidemiological view. *J. Neurol. Neurosurg. Psychiatry* 75, 1376–1381. doi: 10.1136/jnnp.2004.045690
- Leech, R., and Sharp, D. J. (2014). The role of the posterior cingulate cortex in cognition and disease. *Brain J. Neurol.* 137, 12–32. doi: 10.1093/brain/awt162
- Li, X., Morgan, P. S., Ashburner, J., Smith, J., and Rorden, C. (2016). The first step for neuroimaging data analysis: DICOM to NIfTI conversion. *J. Neurosci. Methods* 264, 47–56. doi: 10.1016/j.jneumeth.2016.03.001
- Liegeois-Chauvel, C., Musolino, A., and Chauvel, P. (1991). Localization of the primary auditory area in man. *Brain* 114, 139–151. doi: 10.1093/oxfordjournals.brain.a101854
- Meléndez, J. C., Redondo, R., Escudero, J., Satorres, E., and Pitarque, A. (2019). Executive functions, episodic autobiographical memory, problem-solving capacity, and depression proposal for a structural equations model. *J. Geriatr. Psychiatry Neurol.* 32, 81–89. doi: 10.1177/0891988718824037
- Menary, K., Collins, P. F., Porter, J. N., Muetzel, R., Olson, E. A., Kumar, V., et al. (2013). Associations between cortical thickness and general intelligence in children, adolescents and young adults. *Intelligence* 41, 597–606. doi: 10.1016/j.intell.2013.07.010
- Mitsueda-Ono, T., Ikeda, A., Inouchi, M., Takaya, S., Matsumoto, R., Hanakawa, T., et al. (2011). Amygdalar enlargement in patients with temporal lobe epilepsy. *J. Neurol. Neurosurg. Psychiatry* 82, 652–657. doi: 10.1136/jnnp.2010.206342
- Nee, D. E., Brown, J. W., Askren, M. K., Berman, M. G., Demiralp, E., Krawitz, A., et al. (2013). A meta-analysis of executive components of working memory. *Cereb. Cortex* 23, 264–282. doi: 10.1093/cercor/bhs007
- Novak, A., Vizjak, K., and Rakusa, M. (2022). Cognitive impairment in people with epilepsy. *J. Clin. Med.* 11:267. doi: 10.3390/jcm11010267
- Olejnik, A., Bala, A., Dziedzic, T., Rysz, A., Marchel, A., and Kunert, P. (2024). Executive dysfunction profile in mesial temporal lobe epilepsy. *Acta Neuropsychol.* 22, 1–13. doi: 10.5604/01.3001.0053.9737
- O’Mara, S. M., and Aggleton, J. P. (2019). Space and memory (Far) beyond the hippocampus: Many subcortical structures also support cognitive mapping and mnemonic processing. *Front. Neural Circuits* 13:52. doi: 10.3389/fncir.2019.00052
- Ono, S. E., Mader-Joaquim, M. J., de Carvalho Neto, A., de Paola, L., Dos Santos, G. R., and Silvado, C. E. S. (2021). Relationship between hippocampal subfields and verbal and visual memory function in mesial temporal lobe epilepsy patients. *Epilepsy Res.* 175:106700. doi: 10.1016/j.epilepsyres.2021.106700
- Pail, M., Brázdil, M., Marecek, R., and Mikl, M. (2010). An optimized voxel-based morphometric study of gray matter changes in patients with left-sided and right-sided mesial temporal lobe epilepsy and hippocampal sclerosis (MTLE/HS). *Epilepsia* 51, 511–518. doi: 10.1111/j.1528-1167.2009.02324.x
- Park, C. H., Choi, Y. S., Jung, A. R., Chung, H. K., Kim, H. J., Yoo, J. H., et al. (2017). Seizure control and memory impairment are related to disrupted brain functional integration in temporal lobe epilepsy. *J. Neuropsychiatry Clin. Neurosci.* 29, 343–350. doi: 10.1176/appi.neuropsych.16100216
- Price, C. J. (2010). The anatomy of language: A review of 100 fMRI studies published in 2009. *Ann. N. Y. Acad. Sci.* 1191, 62–88. doi: 10.1111/j.1749-6632.2010.05444.x
- Ptak, R. (2012). The frontoparietal attention network of the human brain: Action, saliency, and a priority map of the environment. *Neurosci. Rev. J. Bringing Neurobiol. Neurol. Psychiatry* 18, 502–515. doi: 10.1177/1073858411409051
- Rayner, G., Jackson, G. D., and Wilson, S. J. (2016). Mechanisms of memory impairment in epilepsy depend on age at disease onset. *Neurology* 87, 1642–1649. doi: 10.1212/WNL.0000000000003231
- Ryvlin, P., Cross, J. H., and Rheims, S. (2014). Epilepsy surgery in children and adults. *Lancet Neurol.* 13, 1114–1126. doi: 10.1016/S1474-4422(14)70156-5
- Siemianowski, C., and Królicki, L. (2005). Znaczenie metod neuroobrazowania w diagnostyce padaczek. *Pol. Przegl. Neurol.* 1, 76–80.
- Skipper, J. I., and Small, S. L. (2006). “fMRI studies of language,” in *Encyclopedia of Language & Linguistics*. Amsterdam: Elsevier Ltd, 496–511. doi: 10.1016/B0-08-044854-2/02399-3
- Vallar, G. (2006). Memory systems: The case of phonological short-term memory. A festschrift for Cognitive Neuropsychology. *Cogn. Neuropsychol.* 23, 135–155. doi: 10.1080/02643290542000012
- Vanneste, S., Mohan, A., De Ridder, D., and To, W. T. (2021). The BDNF Val⁶⁶Met polymorphism regulates vulnerability to chronic stress and phantom perception. *Prog. Brain Res.* 260, 301–326. doi: 10.1016/bs.pbr.2020.08.005

- Wagstyl, K., and Lerch, J. P. (2018). *Cortical Thickness. Brain Morphometry*. Berlin: Springer, 35–49. doi: 10.1007/978-1-4939-7647-8_3
- Wechsler, D. (2009). *Wechsler Memory Scale*, 4th Edn. San Antonio, TX: Pearson.
- Wei, W., Zhang, Z., Xu, Q., Yang, F., Sun, K., and Lu, G. (2016). More severe extratemporal damages in mesial temporal lobe epilepsy with hippocampal sclerosis than that with other lesions: A multimodality MRI study. *Medicine* 95:e3020. doi: 10.1097/MD.0000000000003020
- Whelan, C. D., Altmann, A., Botía, J. A., Jahanshad, N., Hibar, D. P., Absil, J., et al. (2018). Structural brain abnormalities in the common epilepsies assessed in a worldwide ENIGMA study. *Brain J. Neurol.* 141, 391–408. doi: 10.1093/brain/awx341
- Xie, K., Royer, J., Larivière, S., Rodriguez-Cruces, R., Frässle, S., Cabalo, D. G., et al. (2024). Atypical connectome topography and signal flow in temporal lobe epilepsy. *Progr. Neurobiol.* 236:102604. doi: 10.1016/j.pneurobio.2024.102604
- Zhang, Z., Liao, W., Xu, Q., Wei, W., Zhou, H. J., Sun, K., et al. (2017). Hippocampus-associated causal network of structural covariance measuring structural damage progression in temporal lobe epilepsy. *Hum. Brain Mapp.* 38, 753–766. doi: 10.1002/hbm.23415
- Zheng, L., Bin, G., Zeng, H., Zou, D., Gao, J., Zhang, J., et al. (2018). Meta-analysis of voxel-based morphometry studies of gray matter abnormalities in patients with mesial temporal lobe epilepsy and unilateral hippocampal sclerosis. *Brain Imaging Behav.* 12, 1497–1503. doi: 10.1007/s11682-017-9797-5
- Zhou, X., Zhang, Z., Liu, J., Qin, L., Pang, X., and Zheng, J. (2019). Disruption and lateralization of cerebellar-cerebral functional networks in right temporal lobe epilepsy: A resting-state fMRI study. *Epilepsy Behav.* 96, 80–86. doi: 10.1016/j.yebeh.2019.03.020
- Zhu, G., Wang, J., Xiao, L., Yang, K., Huang, K., Li, B., et al. (2021). Memory deficit in patients with temporal lobe epilepsy: Evidence from eye tracking technology. *Front. Neurosci.* 15:716476. doi: 10.3389/fnins.2021.716476
- Zimmer, H. D. (2008). Visual and spatial working memory: From boxes to networks. *Neurosci. Biobehav. Rev.* 32, 1373–1395. doi: 10.1016/j.neubiorev.2008.05.016
- Zubal, R., Velicky Buecheler, M., Sone, D., Postma, T., De Tisi, J., Caciagli, L., et al. (2025). Brain hypertrophy in patients with mesial temporal lobe epilepsy with hippocampal sclerosis and its clinical correlates. *Neurology* 104:e210182. doi: 10.1212/WNL.00000000000210182